A SEMI-QUANTITATIVE MODEL FOR THE BURNING RATE OF SOLID MATERIALS

James G. Quintiere
Department of Fire Protection Engineering
University of Maryland, College Park
MD 20742, USA

ABSTRACT

An analytical model was developed to describe the processes involved in the burning and extinction of solid materials. Included are flame heat transfer, charring, transient conduction, and water application. The model qualitatively describes the burning rate of both charring and thermoplastic-like solids. It illustrates how the steady-state heat of gasification can be derived from peak burning rate test data taken as a function of irradiance. Experimental data are shown to support this derivation. The model, in conjunction with a critical flame temperature, is used to describe suppression and extinction by water.

Keywords: Burn rate, extinction, heat of gasification, model.

1. INTRODUCTION

The degradation of a solid in burning is a complex process. It involves flame heat transfer, evaporation or pyrolysis, possibly charring, and transient thermal effects. Although specific models have been developed, they are limited to classes of materials and do not apply in general. Test apparatuses, such as the Cone Calorimeter, provide a means for dynamically measuring the mass loss and energy release of solid materials, but the interpretation of the data is limited by the lack of a simple model. The purpose of this presentation is to describe a simple model that represents the significant effects in the burning of a solid, and to use that as a potential means for analyzing burning rate data.

2. MODEL

A one dimensional steady stagnant-film approach is used to describe the gas-phase combustion processes. Terms for flame radiation and external radiation are included. In the solid phase, charring, vaporization and transient conduction effects are considered. As vaporization of fuel occurs in the solid it instantaneously is transported to the surface with no resistance through the char layer. A global analysis will be used to describe the solid phase processes which will be linked to the gas-phase by the surface boundary condition. The stagnant film model is available in standard combustion texts (A.M. Kanury, Introduction to Combustion Phenomena, Gordon and Breach, 1977), but is repeated here for completeness. First the solid phase analysis will be considered.

Figure 1 illustrates the model for decomposition in the solid. Vaporization is assumed to occur at a plane behind the char zone. Figure 2 decomposes this model into control volume regions, and displays the heat and mass transfer processes for each region. Measurements are based on the mass loss rate of the solid during burning, so we seek to represent the processes in terms of this quantity. Moreover, the heat of combustion or specie yields derived from measurements are given with respect to the measured mass loss rate. Thus, one may interpret these properties as effective values for the fuel gaseous mixture that leaves the solid. For example, if water vapor is driven off in addition to fuel pyrolyzate, the heat of combustion would represent that of this mixture.

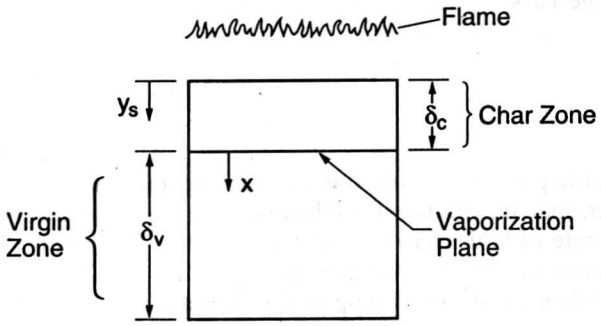

Figure 1. Solid decomposition model

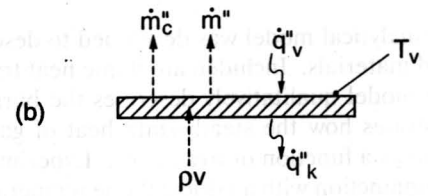

Figure 2b. Vaporization process

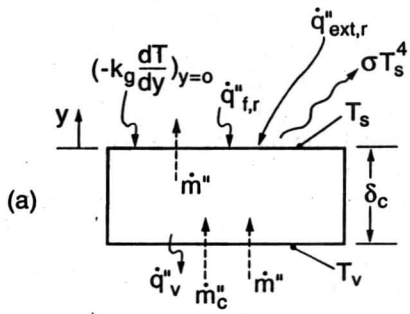

Figure 2a. Char layer process

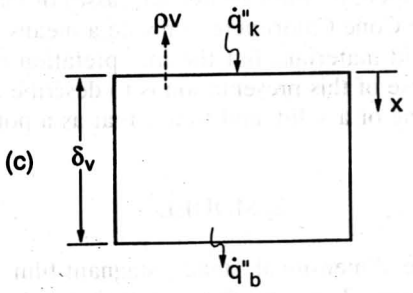

Figure 2c. Virgin material heat transfer processes

2.1 Solid Phase Model

The conservation of mass for the solid in Figure 1 is given by

$$\frac{1}{A}\frac{dm}{dt} + \dot{m}'' = 0 \tag{1}$$

where $\frac{dm}{dt}$ is the mass rate of change of the solid,

A is the surface area,

and $\dot{m}''$ is the mass flow rate of the gasified products per unit area.

Hence, $\dot{m}''$ is the mass loss rate per unit surface area.

By considering the conservations of mass for the char layer in Figure 2a, and assuming that the vaporized fuel instantaneously leaves the solid, it follows that

$$\frac{d}{dt}\int_0^{\delta c} \rho_c \, dy_s = \dot{m}_c'' \tag{2}$$

where ρ_c is the char density, $\dot{m}_c''$ is the mass flow rate per unit area of char from the vaporization plane, and the accumulation of the fuel gases in the char matrix is taken to be negligible. Consequently, a conservation of mass on the virgin fuel element in Figure 2c yields, where the control volume surface moves at the speed of the vaporization plane, $v = \frac{d\delta_c}{dt} = -\frac{d\delta_v}{dt}$, *yields*

$$\frac{d}{dt}\int_{\delta_c}^{\delta_c+\delta_v} \rho \, dy_s + \rho v = 0 \tag{3a}$$

where ρ is the density of the virgin solid. A mass balance at the vaporization plane and Eq.(2), assuming ρ_c is constant, gives

$$\rho v = \dot{m}'' + \dot{m}_c'' = \beta \dot{m}'' \tag{3b}$$

where $\beta = \rho/(\rho-\rho_c)$.

The conservation of energy for each region in Figure 2 is now considered. For the char region (2a),

$$\frac{1}{A}\frac{dU_c}{dt} + \dot{m}'' c_g (T_s - T_v) - \dot{m}_c'' c_c (T_v - T_o) = \left(-k_g \frac{dT}{dy}\right)_{y=o} + \dot{q}_{f,r}'' + \dot{q}_{ext,r}'' - \sigma T_s^4 - \dot{q}_v'' \tag{4}$$

where

U_c is the internal energy of the char layer,

c_g is the specific heat of the vaporized fuel gas,
c_c is the char specific heat,

$-\left(k_g \frac{dT}{dy}\right)_{y=0}$ is the flame convective heat flux,

$\dot{q}''_{f,r}$ is the flame radiative heat flux,
$\dot{q}''_{ext,r}$ is the external radiative flux to the surface,
σT_s^4 is the surface reradiative heat flux (assumed to be a blackbody),
$\dot{q}''_v$ is the heat flux to the plane of vaporization,
and T_o is the reference temperature.

The conservation of energy applied to the vaporization plane of Figure 2b yields:

$$(\rho v)\Delta H_v = \dot{q}''_v - \dot{q}''_k \tag{5}$$

where ΔH_v is the heat of vaporization (pyrolysis) for the solid at temperature T_v,
$\dot{q}''_k$ is the heat loss per unit area to the virgin solid.

The left side of Eq. (5) relates to the energy required to change the virgin solid to vapor and char, and can be taken as a definition of ΔH_v.

An energy balance on the virgin solid gives

$$\frac{1}{A}\frac{dU_v}{dt} + \rho v c(T_v - T_o) = \dot{q}''_k - \dot{q}''_b \tag{6}$$

where $\dot{q}''_b$ is the heat loss per unit area from the back of the solid,
and U_v is the internal energy of the virgin solid.

Since the density (ρ) and specific heat (c) of the virgin solid can be considered constants,

$$U_v = \rho c A \int_{\delta_c}^{\delta_v+\delta_c} (T - T_o)\, dy_s \tag{7}$$

Consider pure conductive heat transfer into the virgin solid with the space coordinate (x), fixed to the moving vaporization plane. If x_o is the initial fixed reference system,

$$x = x_o - \int_o^t v(\tau)\, d\tau \tag{8}$$

where v is the velocity of the vaporization plane. The conduction equation in the fixed frame of reference is

$$\rho c \frac{\partial T}{\partial t} = k \frac{\partial^2 T}{\partial x_o^2} \tag{9}$$

which transforms as

$$\left(\frac{\partial T}{\partial t}\right)_{x_o} = \left(\frac{\partial T}{\partial t}\right)_x + \left(\frac{\partial T}{\partial x}\right)_t \frac{dx}{dt}$$

$$= \left(\frac{\partial T}{\partial t}\right)_x - v\left(\frac{\partial T}{\partial x}\right)_t \tag{10}$$

and

$$\left(\frac{\partial^2 T}{\partial x_o^2}\right)_t = \left(\frac{\partial^2 T}{\partial x^2}\right)_t$$

from Eq. (8). Hence in the moving frame of reference,

$$\rho c \left[\left(\frac{\partial T}{\partial t}\right)_x - v \left(\frac{\partial T}{\partial x}\right)_t\right] = k \left(\frac{\partial^2 T}{\partial x^2}\right)_t \tag{11}$$

with the conditions:

$$x=0,\ -k \frac{\partial T}{\partial x} = \dot{q}_k''$$

$$x=\delta_v,\ -k\frac{\partial T}{\partial x} = \dot{q}_b'' \tag{12}$$

and

$$t=0,\ T=T_o,\ \textit{the initial temperature.}$$

Let us consider the ideal case of a non-charring material undergoing steady burning. If steady conditions prevail in the moving system, i.e., the temperature field is not changing in the virgin solid relative to the moving vaporization plane, and the back face conditions are negligible, i.e., a very thick solid, then Eq. (11) becomes

$$-\rho c v \frac{dT}{dx} = k \frac{d^2T}{dx^2} \tag{13}$$

From Eq. (3) and since $v = -\frac{d\delta_v}{dt}$

$$-\dot{m}'' c \frac{dT}{dx} = k \frac{d^2T}{dx^2} \tag{14}$$

with conditions from Eq. (5) and (12)

$$x=0, \; -k \frac{\partial T}{\partial x} = \dot{q}_v'' - \dot{m}'' \Delta H_v \tag{15a}$$

$$x = 0, \; T = T_v \tag{15b}$$

$$x \to \infty, \; T = T_0 \tag{15c}$$

Using Eqns (15b) and (15c)

$$\frac{T-T_o}{T_v-T_o} = e^{-\frac{c\dot{m}''}{k} x} \tag{16}$$

and from Eq. (15a)

$$\dot{m}'' = \frac{\dot{q}_v''}{\Delta H_v + c(T_v-T_o)} \tag{17}$$

The denominator of Eq. (17) is commonly referred to as the steady state heat of gasification (L_g).

$$L_g = \Delta H_v + c(T_v-T_o) \tag{18}$$

In general, other terms which will be considered below will affect the mass loss rate, $\dot{m}''$. If the process is not steady, we can consider Eq. (11) by integrating each item over δ_v:

$$\int_o^{\delta_v} k\frac{\partial^2 T}{\partial x^2}dx = k\frac{\partial T}{\partial x}\Big|_{x=o}^{x=\delta_v} = \left(-\dot{q}_b''\right) - \left(-\dot{q}_k''\right)$$

$$\rho c\int_o^{\delta_v}\left(-v\frac{\partial T}{\partial x}\right)dx = -c\dot{m}''T\Big|_{x=o}^{x=\delta_v} = -c\dot{m}''\left(T_b - T_v\right)$$

$$\rho c\int_o^{\delta_v}\left(\frac{\partial T}{\partial t}\right)dx = \rho c\frac{d}{dt}\int_o^{\delta_v} T\,dx - \rho cT\left(\delta_v, t\right)\frac{d\delta_v}{dt}$$

$$= \rho c\frac{d}{dt}\int_o^{\delta_v} T\,dx + c\dot{m}''T_b$$

$$= \rho c\frac{d}{dt}\int_o^{\delta_v}\left(T-T_o\right)dx + c\dot{m}''\left(T_b-T_o\right)$$

Also for the charring case since at the vaporization plane

$v = -\frac{d\delta_y}{dt} = \frac{d\delta_c}{dt}$, and from Eq. (3b) it follows that $\dot{m}''$ should be replaced by $\beta\dot{m}''$ in the above.

Substituting in the integrated form of Eq. (11) gives

$$\rho c\frac{d}{dt}\int_o^{\delta_v}\left(T-T_o\right)dx + \beta\dot{m}''c\left(T_b-T_o\right) - \beta\dot{m}''c\left(T_b-T_v\right)$$

$$= \dot{q}_k'' - \dot{q}_b''$$

which is identical to Eq. (6).

From Eq. (5)

$$\rho c\frac{d}{dt}\int_o^{\delta_v}\left(T-T_o\right)dx + \beta\dot{m}''c\left(T_v-T_o\right) = \dot{q}_v'' - \beta\dot{m}''\Delta H_v - \dot{q}_b'' \qquad (19)$$

or

$$\beta\dot{m}''L_g = \dot{q}_v'' - \dot{q}_b'' - \rho c\frac{d}{dt}\int_o^{\delta_v}\left(T-T_o\right)dx.$$

This is a departure from the steady state results given by Eq. (17). It applies to the non-charring case if $\dot{q}_v''$ is regarded as the net surface heat flux, and $\beta = 1$.

The more general charring case is considered by eliminating $\dot{q}_v''$ from Eq. (19) by using Eq. (4). Furthermore, the internal energy of the char is represented as follows:

$\frac{U_c}{A} = \int_o^{\delta_c} \rho_c u_c \, dy_s$ where y_s is measured from the charring surface. The internal energy per unit mass, u_c, is represented as $c_c(T-T_o)$ where c_c is the char specific heat. By Eq. (2) it follows that

$$\frac{1}{A}\frac{dU_c}{dt} = \rho_c c_c \frac{d}{dt}\int_o^{\delta_c} (T-T_o) dy_s \tag{20}$$

From Eq. (4), (19) and (20)

$$\begin{aligned} \beta \dot{m}'' L_g = {} & \left(-k_g \frac{dT}{dy}\right)_{y=o} + \dot{q}''_{f,r} + \dot{q}''_{ext,r} \\ & - \sigma T_s^4 - \rho_c c_c \frac{d}{dt}\int_o^{\delta_c} (T-T_o)\, dy_s - \dot{m}'' c_g (T_s - T_v) \\ & - \dot{q}''_b - \rho c \frac{d}{dt}\int_{\delta_c}^{\delta_v+\delta_c} (T-T_o) dy_s \\ & + \rho_c \beta \dot{m}'' c_c (T_v - T_o) \end{aligned} \tag{21a}$$

Alternatively,

$$\beta \dot{m}'' L_g = \left(-k_g \frac{dT_g}{dy}\right)_{y=o} + \dot{q}''_{f,r} + \dot{q}''_{ext,r} - \sigma T_v^4$$

convective heat transfer — *flame radiation* — *external radiation* — *reradiation (noncharring)*

$$-\sigma\left(T_s^4 - T_v^4\right) - \rho_c c_c \frac{d}{dt}\int_o^{\delta_c} (T-T_o)\, dy_s$$

surface reradiation due to charring — *energy storage due to charring*

$$-\dot{m}'' c_g (T_s - T_v) + \delta_c \beta \dot{m}'' c_c (T_v - T_o)/\rho - \dot{q}''_b \tag{21b}$$

energy flow through char — *back face heat loss*

$$- \rho c \frac{d}{dt}\int_{\delta_c}^{\delta_v} (T-T_o) dy_s$$

virgin solid energy storage

(The above labels are qualitative descriptions of the terms.)

Equation (21b) gives the thermal boundary condition for the gas phase analysis, i.e.,

$$- k_g\left(\frac{dT_g}{dy}\right) = \beta \dot{m}'' \mathcal{L}$$

where

$$\mathcal{L} \equiv L_g + \frac{\rho c \frac{d}{dt} \int_{\delta_c}^{\delta_v+\delta_c} (T-T_0)dy_s + \dot{q}_b'' + \rho_c c_c \frac{d}{dt} \int_0^{\delta_c} (T - T_0)\, dy_s}{\beta \dot{m}''}$$

$$+ \frac{\dot{m}'' c_g (T_s - T_v) - \rho_c \beta \dot{m}'' c_c (T_v - T_o)/\rho + \sigma T_s^4}{\beta \dot{m}''} \qquad (22)$$

$$- \frac{\dot{q}_{f,r}'' + \dot{q}_{ext,r}''}{\beta \dot{m}''}$$

The form in Eq. (22) constitutes a boundary condition for the gas phase problem to follow.

2.2 Flame Model

The gas-phase one dimensional diffusion flame is solved by conventional means (e.g., Kanury [7]). The steady equations are listed below and relate to the diagram in Figure 3:

Conservation of mass:

$$\dot{m}'' = \textit{constant for all } y\,, \qquad (23)$$

Conservation of energy:

$$\dot{m}'' c_g \frac{dT_g}{dy} = k_g \frac{d^2 T_g}{dy^2} - \dot{m}_f''' \Delta H_c (1 - \chi_r)\,, \qquad (24)$$

Conservation of oxygen:

$$\dot{m}'' \frac{dY_{ox}}{dy} = \rho_g D \frac{d^2Y_{ox}}{dy^2} + \dot{m}'''_{ox} \tag{25}$$

All of the fluid properties are assumed constant. D is the diffusion coefficient and the Lewis number, $k_g/\rho_g c_g D$ is assumed equal to one. Stoichiometry gives

$$\dot{m}'''_{ox} = r \dot{m}'''_f \tag{26}$$

where r is the stoichiometric oxygen to fuel mass ratio, $\dot{m}'''_f$ and $\dot{m}'''_{ox}$ are the respective rates of generation per unit volume for fuel and oxygen.

The boundary conditions are given as

$$\begin{aligned} &y = \delta_g, \; T = T_\infty \\ &\quad Y_{ox} = Y_{ox,\infty} \\ &y = 0, \; T = T_s \\ &\quad \frac{dY_{ox}}{dy} = 0, \\ &\quad -k_g \frac{dT_g}{dy} = \dot{m}'' \beta \mathfrak{L} \; Eq. \; (22). \end{aligned} \tag{27}$$

and

and

By introducing a new variable,

$$b = T + \frac{\Delta H_c (1 - \chi_r)}{r c_g} Y_{ox}, \tag{28}$$

based on adding Eqns. (24) and (25) in order to eliminate the chemical source terms it can be shown that

$$\dot{m}'' = \frac{h}{c_g} \ln (1 + B) \tag{29}$$

where

$$B = \frac{Y_{ox,\infty}(1 - \chi_r)\Delta H_c / r + c_g (T_\infty - T_s)}{\beta \mathfrak{L}} \tag{30}$$

and $\frac{k_g}{\delta_g}$ has been replaced by h, a convective heat transfer coefficient.

By introducing

$$\xi = \frac{\dot{m}'' c_g}{h} \tag{31}$$

it can be shown from Eq. (22) that at y = 0

$$- k_g \frac{dT_g}{dy} = \left(\frac{\xi}{e^{\xi}-1}\right) \frac{h}{c_g} \left[Y_{ox,\infty} \frac{\Delta H_c (1-\chi_r)}{r} + c_g (T_\infty - T_s) \right] \tag{32}$$

which is the convective heat flux to the surface. The quantity $\xi/(e^{\xi}-1)$ is called the "blocking factor" which effectively reduces h from its pure heat transfer value as the mass transfer, $\dot{m}''$, increases. Eq. (32) can be combined with Eq. (21b) to give an implicit expression to evaluate $\dot{m}''$, the mass loss rate per unit area of the burning solid. However, the heat flux terms and terms due to charring and transient effects need to have specific values or tractable formulations before a solution can be determined.

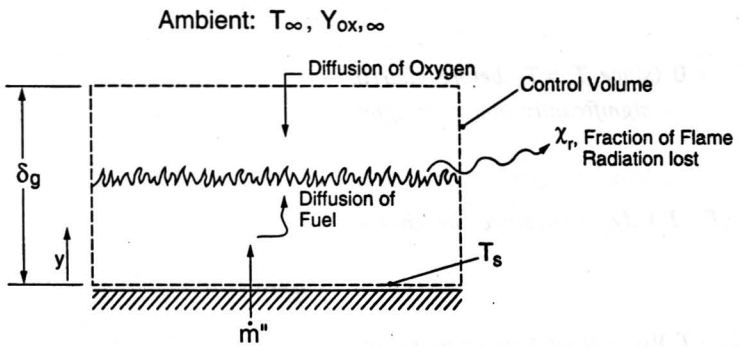

Figure 3. One dimensional diffusion flame system

3. Qualitative Results

Although it is possible to pursue approximate solutions by assuming temperature profiles for the solid, this will not be done. Instead, qualitative analyses will be explored to describe the general burning behavior of solids. Initially, as the solid reaches its vaporization temperature T_v it behaves like a thermoplastic or non-charring material before a significant char layer is developed. To simplify the interpretation it is useful to initially consider the blocking factor and the flame radiant heat flux to be constants. The former will decrease with $\dot{m}''$ while $\dot{q}''_{f,r}$ is likely to increase with $\dot{m}''$ due to an increase in the flame thickness. Both of these effects can be used to temper the descriptions below.

Figure 4 depicts the behavior of the burning rate over time as vaporization ensues after time zero. For a non-charring material, the surface approximately remains at T_v and only the energy storage term in the material affects the burn rate provided the solid is thick so no significant back-face heat loss occurs. As time increases, the energy storage term approaches zero (see Eqs (17) and (19)) as a steady-state is sought. However, once thermal effects are felt at the back-face, the burn rate is disturbed. For a back-face substrate with a lower conductivity than the burning solid, an increase in the burn rate will occur until burn-out of the solid. The opposite effect will result for a higher conductivity substrate.

If charring occurs the behavior is more complex, but describable by Eq. (21b). Initially, the burning begins like the non-charring case. But as the char layer increases, T_s increases and the charring terms in Eq. (21b) all increase to reduce the burning rate. This is shown in Figure 4, again with a corresponding back-face heat loss effect. At the maximum for the charring curve and for the peak of the non-charring curve before back-face effects occur, it can be argued that the following terms are small:

$$\rho c \frac{d}{dt} \int_{\delta_c}^{\delta_v+\delta_c} (T - T_o)\, dy_s \approx 0 \quad (\textit{since we assume}$$

$$\sigma (T_s^4 - T_v^4) \approx 0 \quad (\textit{since } T_s \approx T_v \textit{ before charrin}$$
$$\textit{significantly above its ignit}$$

$$\rho_c c_c \frac{d}{dt} \int_{o}^{\delta_c} (T - T_o)\, dy_s \approx 0 \quad (\textit{since the char l}$$

$$\rho_c \beta \dot{m}'' c_c (T_v - T_o)/\rho = 0 \quad (\textit{if non-charring or}$$

$$\dot{m}'' c_g (T_s - T_v) \approx 0 \quad (\textit{since } T_s \approx T_v)$$

$$\dot{q}_b'' \approx 0 \quad (\textit{since the solid is assumed thermally thick which would}$$
$$\textit{hold in the early stage of burning for materials})$$

Therefore, these peak burning rate conditions, Eq. (21b) can be approximated as

$$\dot{m}''_{max}\ \beta L_g \approx \left(\frac{\xi}{e^{\xi}-1}\right)\frac{h}{c_g}\left[Y_{ox,\infty}\,\Delta H_c(1-\chi_r)/r + c_g(T_\infty - T_v)\right] + \dot{q}''_{f,r} + \dot{q}''_{ext,r} - \sigma T_v^4 \qquad (33)$$

where βL_g can be regarded as the steady state heat of gasification for a charring materials in general.

If in a test apparatus the convective and radiative flame heat fluxes do not vary greatly over a range of peak mass loss rates, then the variation of $\dot{m}''_{max}$ with $\dot{q}''_{ext,r}$ will be linear. The slope is $1/\beta L_g$ and provides an approximate method for determining βL_g. Moreover, if the flame heat fluxes could be determined, Eq. (33) would provide a means for estimating the peak burn rate per unit area for, in principle, all fire conditions. Thus, given βL_g for the material, and a knowledge of the fire heat fluxes, the burning rate can be estimated. This procedure provides a framework for utilizing small scale data such as that developed from the Cone Calorimeter and similar devices.

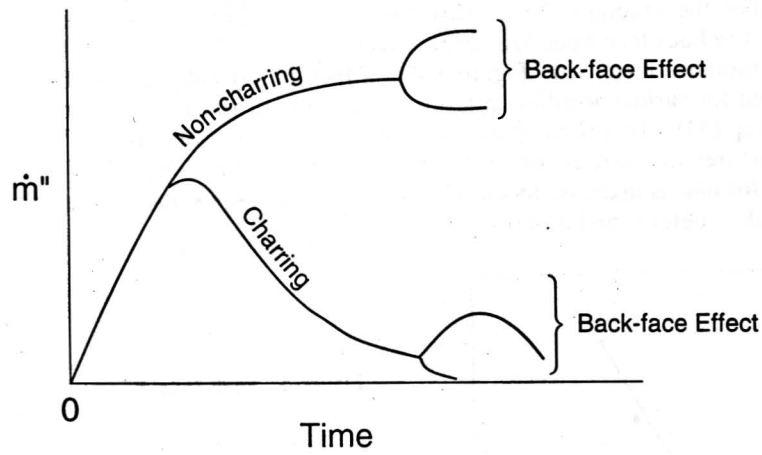

Figure 4. Qualitative description of burning rate for solids

3.1 Examination of Experimental Results

It is generally found that small scale test data for the mass or energy release rate of materials is an approximate linear function of irradiance $\dot{q}''_{ext,r}$. Tewarson [1] has shown this to be the case, and has utilized heating in nitrogen to derive L_g from Eq. (33). In the case of nitrogen, the flame heat transfer terms are non-existent. Jackson [2] performed similar experiments in a nitrogen atmosphere and investigated effects over time. He defined a bulk heat of gasification of the solid as the total net heat added divided by the instantaneous mass loss rate. In terms of Eq. (21), this would correspond in a nitrogen (non-flaming) system as

$$(L_g)_{bulk} = \beta L_g + \rho c \frac{d}{dt} \int_{\delta_c}^{\delta_v+\delta_c} (T - T_o)\, dy_s/\dot{m}'' + \rho_c c_c \frac{d}{dt} \int_{o}^{\delta_c} (T - T_o) dy_s/\dot{m}'' + c_g (T_s - T_v) - \rho_c \beta c_c (T_v - T_o)/\rho \tag{34}$$

Based on our previous discussion, the bulk heat of gasification for a non-charring material would asymptotically approach L_g, the steady value as the energy storage term goes to zero. Jackson, indeed, finds this to occur for PMMA measurements from which yield $L_g)_{bulk}$ as a function of time, but the asymptote depended on the irradiance level. This dependence could have been a result of inaccuracies in his estimation of the back-face heat loss terms as suggested by the fact that the effect on L_g was diminished as the irradiance increased. Figure 5 shows Jackson's results for PMMA in terms of peak mass loss rate plotted for various irradiation levels. The slope of those data yield L_g = 1.89 kJ/g as suggested by using Eq. (33). This is compared to a time asymptotic value at 40 kW/m^2 irradiance of 1.65 kJ/g. This compares to a steady-state value by Tewarson of 1.63 kJ/g [1]. Figure 6 shows peak values of $\dot{m}''$ plotted for oak as taken by Jackson in nitrogen. From the slope of these data, L_g (or more precisely βL_g) for oak is determined as 4.0 kJ/g.

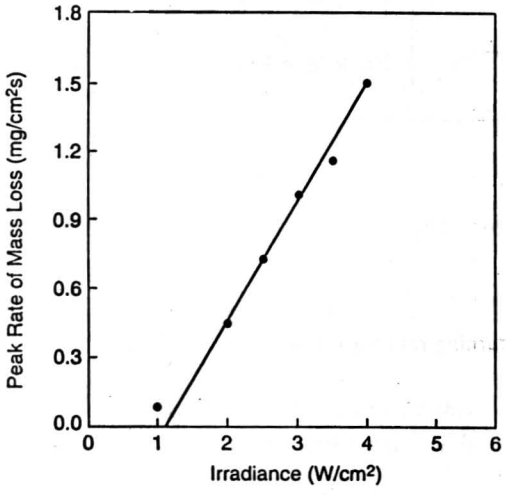

Figure 5. Peak rates of mass loss versus irradiance for PMMA from Jackson [2]

An example of data taken under flaming conditions is presented in Figure 7 for particle board. These samples were tested vertically at a nominal size of 0.3 m high. The data come from Walton and Twilley [3] for irradiances of 25, 50 and 74 kW/m^2, and for 0 irradiance as determined by Kulkarni [4]. Also shown are data from Tsantiadis and Ostman [5] for a particle board material that may not necessarily be identical to that of the other studies. Whether the absolute peak or an average peak value for $\dot{m}''$ is used, the results for L_g range from 4.4 to 4.7 kJ/g. If one applies this technique to a wide range of data for materials used in a series of room fire tests performed in Sweden [5], the L_g values can be determined and are given in Table 1. It is not possible to develop an explanation for the trends of these data, and to explain them in terms of their material composition. The result for L_g can simply be regarded as empirical which allow the prediction of the change in mass loss rate with the change in surface heat flux. However, Eq. (33) gives a physical interpretation to L_g making it the steady-state heat of gasification appropriate to burning a liquid-like fuel. Although this mechanism of pyrolysis will be very different from the evaporation of a liquid, the model being used appears to give a first-order representation of peak mass loss with heat flux in a range of conditions appropriate to common building fires.

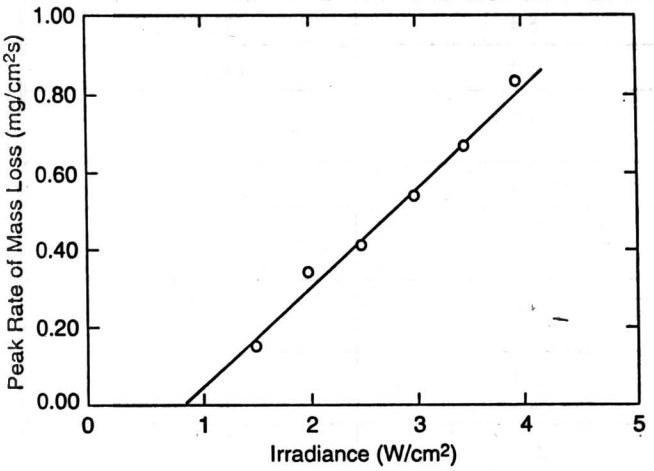

Figure 6. Peak mass loss rate for oak from Jackson [2]

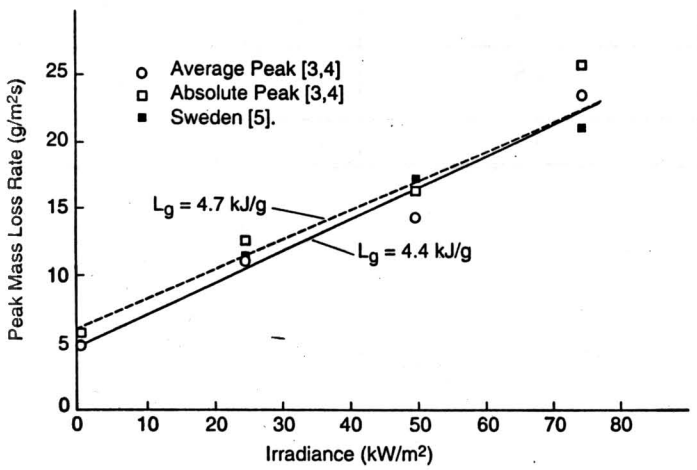

Figure 7. Peak mass loss rate for particle board [3,4,5]

Table 1

Heat of Gasification Values at Peak Burning Conditions

Material	L_g (kJ/g)	Data Source
PMMA	1.89	Jackson [2]
PMMA	1.63	Tewarson [1]
Oak	4.0	Jackson [2]
Particle Board	5.4	[3], [4], [5]
Insulating Fiber Board	4.2	Ostman [5]
Medium Density Fiber Board	4.8	" "
Spruce panel	6.3	" "
Melamine-faced Particle Board	4.8	" "
Paper Wallcovering on Gypsum Board	4.8	" "
Plastic Wallcovering on Gypsum Board	3.7	" "
Paper Wallcovering on Particle Board	6.5	" "
Textile Wallcovering on Gypsum Board	1.5	" "
Textile Wallcovering on Rockwool	2.8	" "
Rigid Polyurethane Foam	3.1	" "

4. EXTINCTION

To close this simplified view of burning, extinction is considered in terms of a critical flame temperature criterion. It is empirically established that for both pre-mixed flames at the lower flammable limit and for diffusion flames at extinction, a minimum flame temperature corresponds to these phenomena. Typically this critical temperature is roughly 1600 K for many C-H-O fuels burning in air (e.q. Williams reports measured values at extinction of 1500 ± 50K [6]). Based on this concept, it can be investigated how the flame temperature in the stagnant film flame model can be reduced through heat losses. Equation (21) can be used as a boundary condition to establish the net heat losses from the flame at the fuel surface. One approach is to return to the stagnant film flame model and solve for the temperature at the flame sheet.

Because we have included more heat transfer processes than would be consistent with the pure convective stagnant film model we must consider the relevance of these fluxes on flame temperature. A control volume approach is taken as shown in Figure 3. The heat and mass transfer processes that directly affect the flame temperature are illustrated in Figure 8. The radiative loss from the flame is accounted for by an effective decrease to the heat of combustion -- yielding less chemical energy available to produce the flame temperature. Therefore, the only heat loss from the flame (control volume) involves the convective heat flux to the fuel surface -- this constitutes $\dot{q}''_{net}$ shown in Figure 8. The other heat fluxes $\dot{q}''_{ext,r}$, to the surface, and σT_s^4, from the surface are considered not to interact with the flame system.

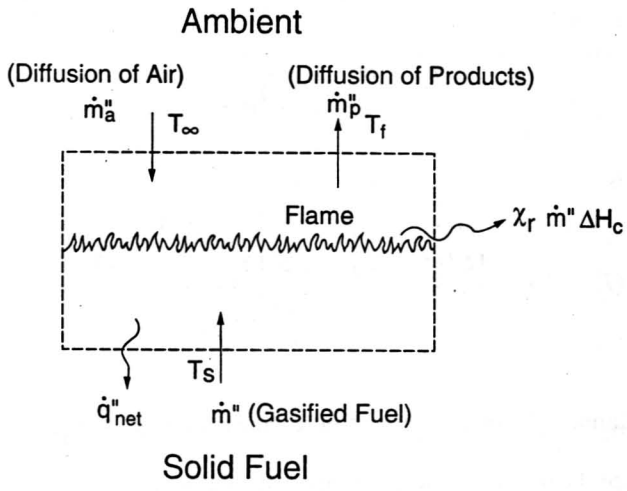

Figure 8. Energy and mass loss streams for diffusion flame

By conservation of mass

$$\dot{m}_p'' = \dot{m}'' + \dot{m}_a'', \tag{35}$$

and by conservation of energy and Eq. (22),

$$\dot{m}_p'' c_g (T_f - T_\infty) - \dot{m}'' c_g (T_s - T_\infty) = \dot{m}'' \Delta H_c (1 - X_r) - \dot{m}'' \beta \mathcal{L}' \tag{36}$$

where $\mathcal{L}' = \mathcal{L} + \dfrac{\dot{q}_{f,r}''}{\beta \dot{m}''}$ by Eq. (22) because the flame heat flux, $\dot{q}''_{f,r}$ has been effectively eliminated in this analysis since all the flame radiative loss is accounted for by χ_r.

Also by stoichiometry:

$$\dot{m}_a'' = \dot{m}'' \frac{r}{Y_{ox,\infty}}$$

and (37)

$$\dot{m}_p'' = \dot{m}'' \left(1 + \frac{r}{Y_{ox,\infty}}\right).$$

Then solving for T_f yields

$$c_g (T_f - T_s) = \frac{[\Delta H_c (1 - X_r) - \beta \mathcal{L}'] Y_{ox,\infty}/r + c_g (T_\infty - T_s)}{1 + Y_{ox,\infty}/r} \tag{38}$$

which can be found in Kanury [7] for the case of pure convection: $\mathcal{L}' = L_g$, $T_s = T_v$ and $X_r = 0$.

The quantities that reduce T_f and drive the flame towards extinction are readily seen:

1. increasing X_r
2. decreasing $Y_{ox,\infty}$
3. decreasing T_∞
4. increasing energy storage due to charring and transient effects in the solid
5. increasing L_g
6. decreasing external radiative heat flux

Extinction by the evaporation of water can also be accounted for by adding $\dot{m}_w'' L_w/\dot{m}''$ to the right side of Eq. (22) if $\dot{m}_w''$ is the mass evaporation rate of water per area of the solid surface and L_w is the heat of gasification of the water (2.6 kJ/g).

As an example of how to apply the temperature criterion consider some simple cases. Take the fuel to be PMMA and ignore all transient and radiative effects. We might expect flame radiative effects to be small near extinction, but not transient and reradiation effects. Hence our result will be illustrative, but approximate. The following properties are used:

c_g = 1 J/gK
T_∞ = 20°C
T_v = 377°C
ΔH_c = 25.2 kJ/g
L_g = 1.63 kJ/g
r = 2 g oxygen/g PMMA

Using T_f = 1600 K, we can estimate the $Y_{ox,\infty}$ to cause extinction of this PMMA flame. Substituting into Eq. (38) yields:

$$(10^{-3})(1600 - 650) = \frac{(25.2 - 1.63)Y_{ox,\infty}/2 + (10^{-3})(293 - 650)}{1 + Y_{ox,\infty}/2}$$

$$Y_{ox,\infty} = \frac{1.376}{4.79} = 0.117,$$

or extinction occurs at a mole fraction of approximately 10.5% oxygen. The corresponding burning rate at extinction in this oxygen atmosphere can be found from Eq. (33) as follows:

Let h = 14 W/m^2K (a typical value corresponding to natural convection) and assume the blocking factor = 1.

$$\dot{m}''_{extinct} = \left\{\frac{h}{c_g}\left[Y_{ox,\infty}\Delta H_c/r + c_g(T_\infty - T_v)\right] - \sigma T_v^4\right\}/L_g$$

where now we include the re-radiation loss.

$$m''_{extinct} = \left\{\left(\frac{14}{1}\right)[0.117\,(25.2)/2 + 10^{-3}\,(293 - 650)\} - 5.67 \times 10^{-11}\,(650)^4\right\} / 1.63$$

or

$$\dot{m}''_{extinct} = 3.4\ g/m^2s.$$

The heat transfer coefficient used above was selected as a plausible value that would lead to a typical value for $\dot{m}''$ found at extinction. Thus, under the condition given above, the PMMA will extinguish in an oxygen environment of 10.5% with a maximum burn rate of 3.4 g/m^2s just before extinction.

By considering all the terms in Eq. (38) we can determine a relationship among the "independent" parameters that must hold at extinction. For example, for fixed values of T_s, $Y_{OX,\infty}$, T_∞, there is a critical value of $\mathcal{L}'$ at extinction (T_f = 1600K).

As another example let us examine the steady burning of PMMA simultaneously exposed to an irradiance ($\dot{q}''_{ext,r}$) and a steady water spray ($\dot{m}''_w$). From Eqns. (22) and (36),

$$\mathcal{L}' = L_g + \frac{\sigma T_v^4 + \dot{m}''_w L_w - \dot{q}''_{ext,r}}{\dot{m}''} \tag{39}$$

Let $Y_{OX,\infty}$ = 0.233, T_∞ = 293 K and the previous PMMA properties. Substituting into Eq. (38) yields

$$10^{-3}(1600 - 650) = \frac{\left\{\left[25.2 - (1.63 + 5.67\times10^{-11}(650)^4 + \dot{m}''_w(2.6) - \dot{q}''_{ext,r}\right]\right\}}{\dot{m}_{extinct}} \tag{40}$$

or

$$\dot{m}''_{extinct} = \frac{2.6\dot{m}''_w + 10.1 - \dot{q}''_{ext,r}}{13.2}$$

From the steady PMMA (non-charring) mass loss Equation (21) with the water term included as $\dot{m}''_w L_w$ on the right side,

$$\dot{m}''L_g = \left(\frac{h}{c_g}\right)\left[Y_{ox,\infty}\Delta H_c(1 - X_r)/r + c_g(T_\infty - T_v)\right] + \dot{q}''_{f,r} + \dot{q}''_{ext,r} - \sigma T_v^4 - \dot{m}''_w L_w$$

where the blocking factor has been taken as one. Here we will take h = 8 W/m^{2}K to match the data for no water application. Ignoring flame radiation loss, yields

$$\dot{m}''(1.63) = \left(\frac{8}{1}\right)\left[0.233(25.2)/2 + 10^{-3}(293 - 650)\right] + \dot{q}''_{ext,r} - 10.1 - 2.6\dot{m}''_w$$

or

$$\dot{m}'' = 6.4 + 0.61\,\dot{q}''_{ext,r} - 1.6\dot{m}''_w \left(\frac{g}{m^2\text{-}s}\right) \tag{41}$$

with $\dot{q}''_{ext,r}$ in kW/m^2. Eq. (41) gives the burning rate under all conditions. Equating this to Eq. (40) gives the relationship holding at extinction:

$$0.20\dot{m}''_w + 0.77 - 0.076\ \dot{q}''_{ext,r} = 6.4 + 0.61\ \dot{q}''_{ext,r} - 1.6\ \dot{m}''_w$$

or

$$\dot{q}''_{ext,r} = 2.6\ \dot{m}''_w - 8.2\ \left(\frac{kW}{m^2}\right) \tag{42}$$

Eq. (42) gives the critical irradiance for a given water spray rate at extinction. The results of Eq. (41) and (42) are in qualitative agreement with the experimental data of Magee and Reitz [8] as shown in Figure 9 with the critical irradiance at extinction underestimated by the theory. Nevertheless, these results show the versatility and level of accuracy of the simple burning rate model presented.

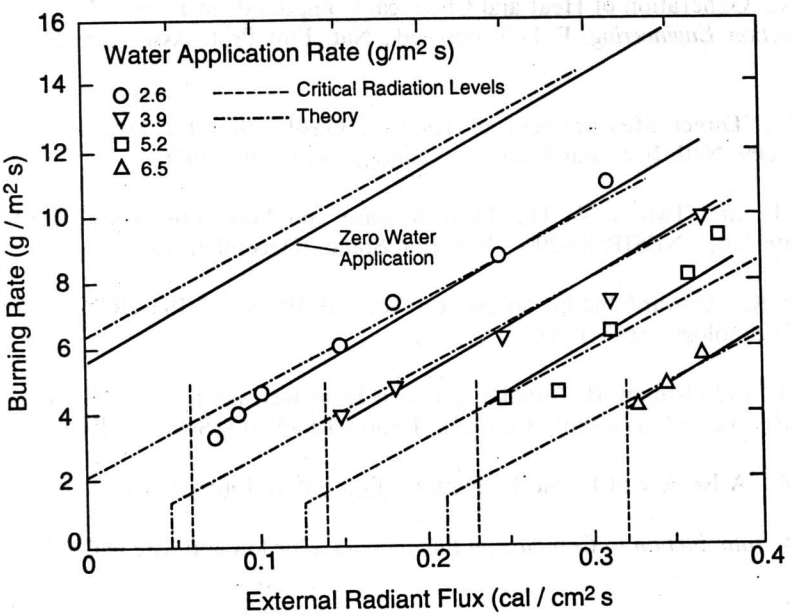

Figure 9. Burning rate of vertical PMMA slabs versus external radiant flux for various water application rates from Magee and Reitz [8]

5. CONCLUSIONS

A simple burning rate model has been developed for a solid which is based on a stagnant film diffusion flame and a control volume formulation for the solid. External irradiance, charring and other transient effects, back-face heat loss and water application are phenomena included. The model is shown to yield results that could have acceptable accuracy for making estimates of burning rate for materials. It is shown that the steady-state heat of gasification could be estimated from small-scale test data by examining the slope of the peak burning rate versus irradiance for both charring and non-charring materials. The terms in the model qualitatively describe the burning rate seen in test data for both charring and non-charring materials. An extinction model based on a critical flame temperature yields results which are qualitatively correct with accuracy that may be sufficient to predict first-order effects.

REFERENCES

1. Tewarson, A., "Generation of Heat and Chemical Compounds in Fires," *The SFPE Handbook of Fire Protection Engineering*, P. DiNenno, ed., Nat. Fire Prot. Assoc.,S.F.P.E., Boston, MA, 1988.

2. Jackson, J.L., "Direct Measurement of Heat of Gasification for Polymethylmethacrylate," NISTIR 88-3809, Natl. Inst. Stand. and Technology, September 1986.

3. Walton, W. D. and Twilley, W. H., "Heat Release and Mass Loss Rate Measurements for Selected Materials," NBSIR 84-2960, Nat. Bur. Stand., December 1984.

4. Kulkarni, A. K., "Upward Flame Spread on Vertical Walls," NIST-GCR-89-565, Natl. Inst. Stand. and Technology, April 1989.

5. Tsantaridis, L. and Ostman, B., "Smoke, Gas and Heat Release Data for Building Products in the Cone Calorimeter," Trateknik Centrum, Report I 8903013, Sweden, 1989.

6. Williams, F.A., "A Review of Flame Extinction", Fire Safety Journal, Vol. 3, 1981.

7. Kanury, A.M., *Introduction to Combustion Phenomena*, Gordon and Breach, Sci. Pub. Inc., New York, 1975.

8. Magee, R.S. and Reitz, R.D., "Extinguishment of Radiation Augmented Plastic Fires by Water Sprays," FMRC Tech. Rept. 22357-1, Factory Mutual Research Corp., Norwood, MA, March 1974.

NOMENCLATURE

A - area
B - Eq. (30)
c - specific test
D - diffusion coefficient
h - convective heat transfer coefficient
k - thermal conductivity
L_g - heat of gasification

L_w - heat of gasification for water
$\mathcal{L}$ - Eq. (22)
$\mathcal{L}'$ - Eq. (36)
m - mass
q - heat transfer
r - stoichiometric oxygen to fuel mass ratio
t - time
T - temperature
u - internal energy per unit mass
U - internal energy
v - velocity
x - coordinate
X_r - radiative fraction of chemical energy
y - coordinate
Y_{ox} - oxygen mass fraction
β - density ratio, Eq. (3b)
δ - thickness
ΔH_c - heat of combustion
ΔH_v - heat of vaporization
ρ - density
ξ - Eq. (31)

Subscripts

b - backface
c - char
ext - external
f - flame
g - gas
k - conduction
o - reference state
p - products
s - solid, surface
v - vaporization, virgin
w - water
∞ - ambient

Superscripts

$(\dot{})$ - per unit time
$(\,)''$ - per unit area
$(\,)'''$ - per unit volume